Quantum Optical Coherent State Discrimination

Paul J. Martin

A thesis submitted to the Department of Physics and Astronomy at the University of New Mexico

Abstract

Calculated optimal quantum measurements are often very challenging to perform in real life because of the inherent difficulty in constructing an optimum superposition-state measurement basis. This thesis demonstrates the viability of employing real-time quantum feedback to physically achieve an optimal measurement. During a simple binary state discrimination process, coherent optical quantum states are displaced according to an optimal feedback solution. The resulting probability of measurement error beats that of merely photon counting, called the shotnoise limit, and approaches the true limit imposed by quantum mechanics, discovered by Helstrom more than thirty years ago.

Publications resulting from this work:

- "Optical coherent state discrimination using a closed-loop quantum measurement," Robert L. Cook, Paul J. Martin, and JM Geremia, *Nature*, **446**, 774-777 (2007).

Contents

List of Figures

Chapter 1

Introduction

A convenient way to think about quantum mechanics is as an information science. From this frame of mind, admitting fundamental quantum properties, such as uncertainty principles and invasive measurements, amounts to understanding that *complete* knowledge of a quantum system is often unattainable [1, 2]. We are limited in our understanding of a quantum system or state for various reasons, but a particularly interesting source of our ignorance is the invasive nature of measurements. From an information perspective, a measurement is any process that allows a gain in knowledge. During the process of a measurement, seemingly delicate quantum states are altered in a nondeterministic, irreversible manner [3]. This means that we cannot repeatedly measure a state to learn everything there is to know about it; if we are given a single copy of a quantum system and the goal to determine its state as accurately as possible, we only have one chance to expand our knowledge through measurement [4].

1.1 Motivation

In quantum mechanics, a fundamental problem lies in extracting information contained in a quantum state. A simple first step in this process is to identify an unknown state, or, more specifically, to distinguish between quantum states [5].

We can try to do this through measurement, but, since the information gain enabled by quantum measurement is limited, we need to employ the *best possible* measurement [1, 6].

When attempting to learn about a quantum system, it is usually possible to optimize over the set of feasible quantum measurements. However, the result is usually very difficult, and often nigh impossible, to implement in real life [7, 8].

This thesis is about finding and implementing an alternative way to perform optimal quantum measurements, where information gain remains maximized and physical realization becomes viable. We use the concept of performing feedback [9, 10, 11, 12, 13] on a quantum system while it is being measured.

1.2 Quantum States

A quantum state $|\psi\rangle$ can conveniently be thought of as a collection of information about a quantum system. A state vector is represented by a superposition of orthogonal basis vectors,

$$|\psi\rangle = \sum_{i=1}^{N} c_i |\phi_i\rangle, \quad \text{such that} \quad \sum_{i=1}^{N} |c_i|^2 = 1. \tag{1.1}$$

The statement that the squared complex coefficients add to one is equivalent to saying $|\psi|^2 = 1$, which is a normalized probability distribution. Indeed, seeing that $|\psi\rangle$ is nearly a probability distribution helps us to understand it a little better—it is a mathematical object that can be used to calculate the probabilities of measurement outcomes. The normalization condition is simply the statement that when $|\psi\rangle$ is measured, an outcome must occur.

Since $|\psi\rangle$ can be decomposed into orthogonal basis vectors, it is called a *pure state*. Often, however, a quantum state can be a statistical mixture of pure states. This *mixed state* is given by the density operator,

$$\hat{\rho} = \sum_{i=1}^{N} c_i |\psi_i\rangle\langle\psi_i|. \tag{1.2}$$

The condition of normalization applies to this form of a quantum state as well, $\mathrm{tr}\hat{\rho} = 1$.

In the absence of a measurement, the quantum state of a system evolves deterministically according to a smooth, unitary operator $\hat{U}(t)$. For pure states, this evolution has the form

$$|\psi(t)\rangle = \hat{U}(t)|\psi(0)\rangle, \quad \text{where} \quad \hat{U}(t) = e^{-i\hat{H}t/\hbar}; \tag{1.3}$$

while for density operators,

$$\hat{\rho}(t) = \hat{U}^{\dagger}(t)\hat{\rho(0)}\hat{U}(t) \tag{1.4}$$

This evolution is simply the dynamics that derive from the time-dependent Schrödinger equation. The transformation performed on quantum state $|\psi(0)\rangle$ by $\hat{U}(t)$ is reversible since $\hat{U}^{\dagger}(t)\hat{U}(t) = \hat{1}$. Because of these properties of unitary evolution, quantum states are classically well-behaved until a measurement is made.

1.3 Quantum Measurements

When a measurement is made on a quantum state, the state changes in a way that is not deterministic. Quantum state reduction, sometimes called the "collapse of the wave function," is the process by which an initial quantum state $|\psi(0)\rangle$ is transformed to its post-measurement state $|\psi'\rangle$. Outcomes of measurements are random, but follow the probability distribution contained in a quantum state.

1.3.1 Projective Measurements

The most simple treatment of measurement, and the one typically learned in any undergraduate course in quantum mechanics, is to associate a Hermitian operator $\hat{M} = \hat{M}^{\dagger}$ with every physical observable of the system. All Hermitian operators can be expressed in terms of their spectral decomposition,

$$\hat{M} = \sum_{i=1}^{N} \lambda_i |m_i\rangle\langle m_i|, \tag{1.5}$$

where the λ_i are the possible measurement outcomes for the physical observable associated with the operator $\hat{A}$. The measurement outcomes λ_i and their associated kets $|m_i\rangle$ are eigenvalues and eigenvectors, respectively,

$$\hat{M}|m_i\rangle = \lambda_i|m_i\rangle. \tag{1.6}$$

The invasive property of quantum measurements is treated by conditioning the state of the quantum system on the outcome of the measurement using projection operators. Each

projector is an outer product of its corresponding eigenvector with itself, $\mathbf{P}_i = |m_i\rangle\langle m_i|$. Projectors are complete,

$$\sum_{i=1}^{N} \mathbf{P}_i = \mathbb{1}, \tag{1.7}$$

and are required to be both *idempotent* and orthogonal,

$$\mathbf{P}_i^2 = \mathbf{P}_i \quad \text{and} \quad \mathbf{P}_i\mathbf{P}_j = \delta_{ij}. \tag{1.8}$$

Thus, projectors correspond to mutually exclusive measurement outcomes.

According to standard quantum mechanics, a measurement corresponds to projecting the quantum state vector $|\psi\rangle$ just prior to the measurement onto the eigenbasis of the operator $\hat{M}$. A projective measurement leaves the quantum state of a system in the eigenstate of the operator corresponding to the measurement eigenvalue obtained

$$|\psi\rangle \mapsto |\psi'\rangle = \frac{\mathbf{P}_i}{\sqrt{\langle\psi|\mathbf{P}_i|\psi\rangle}}|\psi\rangle. \tag{1.9}$$

If measured again, the outcome will remain in the same eigenstate, which means that complete information is gained.

The probability to measure a quantum state $|\psi\rangle$ and observe the outcome λ_i is given by the Born rule,

$$\mathbb{P}(\lambda_i) = |\langle\psi|m_i\rangle|^2 = \langle\psi|\mathbf{P}_i|\psi\rangle. \tag{1.10}$$

The projector $\mathbf{P}_i$ is the observable that corresponds to how likely it is that performing a measurement of $\hat{M}$ will produce the outcome λ_i.

1.3.2 Positive Operator Valued Measures

More general than projective measurements, positive operator valued measures (POVMs) are not necessarily projective. They are partial measurements that are not required to leave the state of the quantum system in an eigenstate of the measurement.

A POVM consists of a complete set of operators that are unlike projectors in that they are not necessarily orthogonal [14, 15]:

$$\mathcal{M} \equiv \{\mathbf{M}_1, \mathbf{M}_2, \ldots, \mathbf{M}_N\}. \tag{1.11}$$

Each $\mathbf{M}_i$ is associated with a measurement outcome i. If N is the number of possible measurement outcomes, then N operators are needed to form a complete POVM. However, since orthogonality is not required, more than N operators may exist in a POVM.

POVMs are the most general class of measurements allowed by quantum mechanics; if a measurement is to be considered allowable, it must meet a few requirements. First, all $\mathbf{M}_i$ components must be strictly positive,

$$\mathbf{M}_i \geq 0 \ \ \forall \mathbf{M}_i. \tag{1.12}$$

This is the condition for the "positive" part of the acronym; it means both that the eigenvalues of the $\mathbf{M}_i$s are nonnegative and that they take positive operators to positive operators. An operator with negative eigenvalues is not considered valid because this implies negative probabilities, which is absurd.

Second, the components must be complete, that is

$$\sum_{i=1}^{N} \mathbf{M}_i = \mathbb{1}. \tag{1.13}$$

This ensures that $\mathcal{M}$ takes normalized states to normalized states, a statement of the conservation of probability, or, equivalently, the trace of the density matrix. If the elements did not resolve the identity, then some measurement outcome would be unaccounted for.

These two requirements ensure that $\mathcal{M}$ takes a valid density operator to another valid density operator. Combined, they are the most general requirements for a process that is allowed by quantum mechanics. POVMs, therefore, are the most general class of allowable quantum measurements.

The "measure" part has to do with probability—the probability to observe the outcome corresponding to the i^{th} element of $\mathcal{M}$ is given by

$$\mathbb{P}(i) = \mathrm{tr}[\mathbf{M}_i \hat{\rho}]. \tag{1.14}$$

1.3.3 Continuous Quantum Measurement and Feedback

Another type of measurement, which will play an important role in this thesis, involves observation and manipulation of a system as it is being measured. This combines unitary

evolution of the quantum state with a measurement conditioning on the same time scale—called a *continuous quantum measurement* [9, 13, 16, 17]. The basic idea is to drive the dynamics of the system over small time increments. In this process, an initial quantum state is transformed into its new form by

$$|\psi(t)\rangle = \lim_{n\to\infty} \left[\mathbf{M}_n \hat{U}_n(\delta t)\mathbf{M}_{n-1}\hat{U}_{n-1}(\delta t) \times \cdots \times \mathbf{M}_2\hat{U}_2(\delta t)\mathbf{M}_1\hat{U}_1(\delta t)\right] |\psi(0)\rangle, \tag{1.15}$$

where $\delta t = \tau/n$. In the continuous limit,

$$|\psi(t)\rangle = \mathbf{M}_t\hat{U}_t(\delta t)\mathbf{M}_{t-dt}\hat{U}_{t-dt}(dt) \times \cdots \times \mathbf{M}_{2dt}\hat{U}_{2dt}(dt)\mathbf{M}_{dt}\hat{U}_{dt}(dt)|\psi(0)\rangle. \tag{1.16}$$

The outcome of the continuous measurement is called the *measurement record* and consists of the full history of measurement data obtained at each point in time

$$\Xi_{[0,t]} = (\lambda_t, \lambda_{t-dt}, \ldots, \lambda_{2dt}, \lambda_{dt}) \tag{1.17}$$

This history is on the same time scale as measurements performed on the quantum system. This mixes up the two traditionally separate roles of smooth evolution according to the Schrödinger equation and nondeterministic measurement.

The idea behind quantum feedback control is that the evolution at a given point in time $\hat{U}_t(dt)$ can be made to depend upon the measurement history $\Xi_{[0,t)}$ prior to time t. In this way, it is possible to exert control over the statistics of the continuous measurement.

1.4 Quantum Hypothesis Testing

Often, we want to ask a question about a quantum state and attempt to answer this question after making some sort of measurement. A *hypothesis testing procedure* is simply the process of associating a guess with a possible measurement outcome [4]. Suppose there are N different guesses that can be made. Our set of hypotheses is

$$\mathcal{H} = \{\mathcal{H}_1, \mathcal{H}_2, \ldots, \mathcal{H}_N\}. \tag{1.18}$$

If we guess $\mathcal{H}_i$, what is the chance that our hypothesis is right? It makes more sense to think about the chance of it being wrong—the probability of error. The probability of error

is simply

$$\mathbb{P}_E = \sum_{i \neq j} \mathbb{P}\left(\mathcal{H}_i | \mathcal{H}_j\right) \mathbb{P}\left(\mathcal{H}_j\right). \tag{1.19}$$

The conditional probabilities $\mathbb{P}\left(\mathcal{H}_i|\mathcal{H}_j\right)$ refer to the chance that we select $\mathcal{H}_i$ when $\mathcal{H}_j$ was correct. They are weighted in the sum by the probability that $\mathcal{H}_j$ was right in the first place.

This possibility of error can be calculated explicitly when defined measurement outcomes are associated with the hypotheses. Quantum hypothesis testing can be considered for a wide variety of inquiries, but this paper is only concerned with the question of state discrimination.

1.4.1 State Discrimination

The question of quantum state discrimination is easily posed. Suppose a quantum state is secretly prepared into one of a set of N possible candidate states. Now, which state is it? The list of candidate states is referred to as an *alphabet*,

$$\mathcal{A} = \left(\hat{\rho}_1, \hat{\rho}_2, \ldots, \hat{\rho}_N\right), \tag{1.20}$$

and we define our hypothesis $\mathcal{H}_i$ to correspond to i^{th} element of this list, $\hat{\rho}_i$.

In addition to the alphabet, we are provided with a complete set of *a priori* probabilities.

$$\mathbb{P}\left(\hat{\rho}_i\right) = p_i \quad , \quad \sum_i^N p_i = 1 \tag{1.21}$$

Thus, the probability of error is easily calculable:

$$\mathbb{P}_E = \sum_{i \neq j} \mathbb{P}\left(\mathcal{H}_i | \hat{\rho}_j\right) p_j. \tag{1.22}$$

If we want to have the greatest chance of being correct (suppose we win a substantial prize if we are right), then we need to minimize this decisional error [1, 5]. We can do this by choosing the measurement we make before selecting our hypothesis; to truly minimize this error, we allow our measurement to take on the general form of a POVM. This is explored in detail in the following pages for the binary case of state discrimination, $N = 2$.

Chapter 2

Binary Optical State Discrimination

In the binary case of state discrimination, we are provided with a list of two unique candidate states that are not necessarily orthogonal. Our alphabet is then given by

$$\mathcal{A} = \{\hat{\rho}_1, \hat{\rho}_2\}. \tag{2.1}$$

We will be given a state that has been chosen from this alphabet according to a probability distribution that is also available to us:

$$\mathbf{p} = \{p_1, p_2\}, \quad p_1 + p_2 = 1. \tag{2.2}$$

Thus, we know that the unknown provided state can be either $\hat{\rho}_1$ or $\hat{\rho}_2$, and the likelihood of being in each state is p_1 or p_2, respectively. The objective is to use this *a priori* knowledge to best determine which state was actually given to us. We are allowed to do anything we want to the state to better determine which candidate state it is; the preservation of the provided state is not considered important in this problem because we are only concerned with identifying it [5].

2.1 Probability of Error

After we have played with the state, presumably by a measurement of some sort, we use our new knowledge of the system to guess which state we were given. Elements in our set of hypotheses [4, 5],

$$\mathcal{H} = \{\mathcal{H}_1, \mathcal{H}_2\}, \tag{2.3}$$

correspond to the two candidate states. A guess is made and can easily be evaluated as either right or wrong: When we choose the state that was not provided, we say that an error occurs—expressed conveniently by the conditional probabilities

$$\mathbb{P}(\mathcal{H}_2|\hat{\rho}_1) \quad \text{and} \quad \mathbb{P}(\mathcal{H}_1|\hat{\rho}_2). \tag{2.4}$$

The total probability of error, according to Eq. (1.19), is found by simply weighting these conditional probabilities with their *a priori* probabilities and adding them together according to Bayes' rule:

$$\mathbb{P}_E = \mathbb{P}(\mathcal{H}_2|\hat{\rho}_1)p_1 + \mathbb{P}(\mathcal{H}_1|\hat{\rho}_2)p_2. \tag{2.5}$$

Clearly, obtaining the best chance of selecting the correct state amounts to minimizing the above probability of error. This is not to difficult to do, but some more machinery is required.

As indicated above, we will attempt to attain more information about the mystery state by performing some sort of measurement. The outcome of our measurement leads to the hypothesis $\mathcal{H}_1$ or $\mathcal{H}_2$. Because we want to see how well we can do in principle, we consider the most general class of allowable measurements in quantum mechanics: POVMs. Since two outcomes are possible, a two-component POVM is sufficient as the general form of measurement:

$$\mathcal{M} = \{\mathbf{M}_1, \mathbf{M}_2\}. \tag{2.6}$$

In order to be an allowable quantum measurement, the matrices $\mathbf{M}_1$ and $\mathbf{M}_2$ are required to be both complete and positive,

$$\mathbf{M}_1 + \mathbf{M}_2 = \mathbb{1}, \quad \mathbf{M}_i \geq \mathbf{0} \ \ \forall \mathbf{M}_i. \tag{2.7}$$

Our hypothesis testing procedure is the following: When the measurement outcome corresponds to $\mathbf{M}_1$, we choose hypothesis $\mathcal{H}_1$, and we make a similar conclusion in the opposite measurement outcome. We can now express the probability of error in Eq. (2.5) in a more useful form, where the conditional probabilities are rewritten using elements of our POVM. Also applying the fact that $\mathbf{M}_1$ and $\mathbf{M}_2$ resolve the identity, we can make the following simplifications:

$$\mathbb{P}_E \quad = \quad \mathbb{P}(\mathcal{H}_2|\hat{\rho}_1)p_1 + \mathbb{P}(\mathcal{H}_1|\hat{\rho}_2)p_2$$

$$\begin{aligned} &= \mathrm{tr}[\mathbf{M}_2\hat{\rho}_1]p_1 + \mathrm{tr}[\mathbf{M}_1\hat{\rho}_2]p_2 \\ &= \mathrm{tr}[(\mathbb{1} - \mathbf{M}_1)\hat{\rho}_1]p_1 + \mathrm{tr}[\mathbf{M}_1\hat{\rho}_2]p_2 \\ &= p_1 - \mathrm{tr}[\mathbf{M}_1\hat{\rho}_1]p_1 + \mathrm{tr}[\mathbf{M}_1\hat{\rho}_2]p_2 \\ &= p_1 + \mathrm{tr}[\mathbf{M}_1\hat{\rho}_2 p_2 - \mathbf{M}_1\hat{\rho}_1 p_1]. \end{aligned} \tag{2.8}$$

Thus, the probability of error is simply

$$\mathbb{P}_E = p_1 + \mathrm{tr}[\mathbf{M}_1\hat{\Gamma}], \quad \text{where} \quad \hat{\Gamma} = p_2\hat{\rho}_2 - p_1\hat{\rho}_1. \tag{2.9}$$

Since $\hat{\Gamma}$ is a linear combination of Hermitian density operators, it is itself Hermitian. This means we can consider its spectral decomposition, given by breaking $\hat{\Gamma}$ apart into its eigenvalues and their associated projectors:

$$\hat{\Gamma} = \sum_j \gamma_j |j\rangle\langle j|, \quad \hat{\Gamma}|j\rangle = \gamma_j|j\rangle. \tag{2.10}$$

Now,

$$\mathrm{tr}[\mathbf{M}_1\hat{\Gamma}] = \sum_i \sum_j \gamma_j \langle i|\mathbf{M}_1|j\rangle\langle j|i\rangle \tag{2.11}$$

$$= \sum_j \gamma_j \langle j|\mathbf{M}_1|j\rangle. \tag{2.12}$$

Since $0 \leq \mathbf{M}_1 \leq \mathbb{1}$, as required by the definition of the POVM, we can say that the above trace is bounded below by the sum of its negative eigenvalues,

$$\mathrm{tr}[\mathbf{M}_1\hat{\Gamma}] \geq \sum_{\gamma_j \leq 0} \gamma_j. \tag{2.13}$$

In this instance, $\hat{\Gamma}$ is neither positive- nor negative-definite because $-\mathbb{1} \leq \hat{\Gamma} \leq \mathbb{1}$. More specifically, there are two eigenvalues, one positive and one negative. Thus, we can say that the value of the trace has a minimum that is equal to γ_-, the negative eigenvalue of $\hat{\Gamma}$. Now, our probability of error has a lower bound—exactly the minimization we were seeking:

$$\mathbb{P}_E = p_1 + \mathrm{tr}[\mathbf{M}_1\hat{\Gamma}] \tag{2.14}$$

$$\geq p_1 + \gamma_-. \tag{2.15}$$

In the case where $\mathbb{P}_E = p_1 + \gamma_-$, we have reached the quantum limit for probability of error, sometimes referred to as the Helstrom bound, p_H. We reach this minimum when we choose

the correct basis in which to measure. We, therefore, choose $\mathbf{M}_1$ such that it corresponds with the eigenvector associated with γ_-:

$$\mathbf{M}_1 = |-\rangle\langle -|, \quad \text{where} \quad \hat{\Gamma}|-\rangle = \gamma_-|-\rangle. \tag{2.16}$$

2.1.1 Derivation of the Quantum Error Limit

In order to find an explicit representation of p_H, that is to say a closed form expression, it is necessary to consider the case where $\hat{\rho}_1 = |\psi_1\rangle\langle\psi_1|$ and $\hat{\rho}_2 = |\psi_2\rangle\langle\psi_2|$ [5]. In this pure state configuration, we simply need to find the negative eigenvalue of

$$\begin{aligned} \hat{\Gamma} &= p_2\hat{\rho}_2 - p_1\hat{\rho}_1 & (2.17)\\ &= p_2|\psi_2\rangle\langle\psi_2| - p_1|\psi_1\rangle\langle\psi_1|. & (2.18) \end{aligned}$$

It would be convenient to express $\hat{\Gamma}$ as a matrix; however, we should remember that $|\psi_1\rangle$ and $|\psi_2\rangle$ are not necessarily orthogonal. We can use our state vectors to construct an orthonormal basis through the method of Gram-Schmidt orthogonalization. Keeping $|\psi_1\rangle$ in our new basis, the un-normalized orthogonal state $|\xi^\perp\rangle$ is given by

$$|\xi^\perp\rangle = |\psi_2\rangle - \frac{\langle\psi_1|\psi_2\rangle}{\langle\psi_1|\psi_1\rangle}|\psi_1\rangle. \tag{2.19}$$

After normalizing $|\xi^\perp\rangle$ we get $|\psi_1^\perp\rangle$, and our new orthonormal basis is complete:

$$|\psi_1\rangle = |\psi_1\rangle, \quad |\psi_1^\perp\rangle = \frac{|\psi_2\rangle - |\psi_1\rangle\langle\psi_1|\psi_2\rangle}{\sqrt{1-|\langle\psi_1|\psi_2\rangle|^2}}. \tag{2.20}$$

Let's expand $\hat{\Gamma}$ in this new basis by calculating $|\psi_2\rangle\langle\psi_2|$. In doing this, let $\alpha = \sqrt{1-|\langle\psi_1|\psi_2\rangle|^2}$ so that $|\psi_2\rangle = \alpha|\psi_1^\perp\rangle + |\psi_1\rangle\langle\psi_1|\psi_2\rangle$. Remembering that $|\langle\psi_1|\psi_2\rangle|^2 + |\langle\psi_1^\perp|\psi_2\rangle|^2 = 1$, the algebra is straightforward:

$$\begin{aligned} |\psi_2\rangle\langle\psi_2| &= |\alpha|^2|\psi_1^\perp\rangle\langle\psi_1^\perp| + \alpha^*\langle\psi_1|\psi_2\rangle|\psi_1\rangle\langle\psi_1^\perp| \\ &\quad +\alpha\langle\psi_2|\psi_1\rangle|\psi_1^\perp\rangle\langle\psi_1| + |\langle\psi_1|\psi_2\rangle|^2|\psi_1\rangle\langle\psi_1| & (2.21)\\ &= \begin{pmatrix} |\langle\psi_1|\psi_2\rangle|^2 & \alpha^*\langle\psi_1|\psi_2\rangle \\ \alpha\langle\psi_2|\psi_1\rangle & |\alpha|^2 \end{pmatrix} & (2.22)\\ &= \begin{pmatrix} |\langle\psi_1|\psi_2\rangle|^2 & \langle\psi_1|\psi_2\rangle\langle\psi_1^\perp|\psi_2\rangle \\ \langle\psi_1|\psi_2\rangle\langle\psi_2|\psi_1^\perp\rangle & |\langle\psi_1^\perp|\psi_2\rangle|^2 \end{pmatrix}. & (2.23) \end{aligned}$$

Thus, we can write $\hat{\Gamma}$ as

$$\hat{\Gamma} = \begin{pmatrix} p_2|\langle\psi_1|\psi_2\rangle|^2 - p_1 & p_2\langle\psi_1|\psi_2\rangle\langle\psi_1^\perp|\psi_2\rangle \\ p_2\langle\psi_1|\psi_2\rangle\langle\psi_2|\psi_1^\perp\rangle & p_2|\langle\psi_1^\perp|\psi_2\rangle|^2 \end{pmatrix}. \tag{2.24}$$

In order to find the negative eigenvalue of $\hat{\Gamma}$, we observe that $\mathrm{tr}\hat{\Gamma} = p_2 - p_1$ and $\det\hat{\Gamma} = -p_1p_2|\langle\psi_1^\perp|\psi_2\rangle|^2$ and utilize a handy formula for computing eigenvalues of a two-by-two matrix,

$$\gamma_\pm = \frac{1}{2}\left(\mathrm{tr}\hat{\Gamma} \pm \sqrt{(\mathrm{tr}\hat{\Gamma})^2 - 4\det\hat{\Gamma}}\right) \tag{2.25}$$

$$= \frac{1}{2}\left(p_2 - p_1 \pm \sqrt{(p_2-p_1)^2 + 4p_1p_2|\langle\psi_1^\perp|\psi_2\rangle|^2}\right). \tag{2.26}$$

Now use the statement of probability, $p_1 + p_2 = 1$, to simplify further

$$\gamma_\pm = \frac{1}{2}\left(1 - 2p_1 \pm \sqrt{1 - 4p_1 + 4p_1^2 + 4p_1p_2|\langle\psi_1^\perp|\psi_2\rangle|^2}\right) \tag{2.27}$$

$$= \frac{1}{2}\left(1 \pm \sqrt{1 - 4p_1 + 4p_1 - 4p_1p_2 + 4p_1p_2|\langle\psi_1^\perp|\psi_2\rangle|^2}\right) - p_1 \tag{2.28}$$

$$= \frac{1}{2}\left(1 \pm \sqrt{1 - 4p_1p_2(1 - |\langle\psi_1^\perp|\psi_2\rangle|^2}\right) - p_1 \tag{2.29}$$

$$= \frac{1}{2}\left(1 \pm \sqrt{1 - 4p_1p_2|\langle\psi_1|\psi_2\rangle|^2}\right) - p_1. \tag{2.30}$$

So, with our *a priori* knowledge of the binary state discrimination problem, we can explicitly compute our probability of error in the *best possible case*—as good as allowed by quantum mechanics. This is our important result:

$$p_H = p_1 + \gamma_- = \frac{1}{2}\left(1 - \sqrt{1 - 4p_1p_2|\langle\psi_1|\psi_2\rangle|^2}\right). \tag{2.31}$$

An additional interesting calculation can be made: the optimum basis for measurement. This is γ_-'s associated eigenvector $|-\rangle$, discussed earlier. Plugging directly into the eigenvalue equation $\hat{\Gamma}|-\rangle = \gamma_-|-\rangle$ and solving for $|-\rangle$ proves ugly, but is simplified greatly by assuming *a priori* probabilities $p_1 = p_2 = \frac{1}{2}$. This equal probability case is actually very interesting because it has the highest probability of error as well as the highest potential to communicate information [2]. With this simplification, the un-normalized eigenvector is given by

$$|-\rangle = \left(2\langle\psi_1|\psi_2\rangle - \frac{\langle\psi_1|\psi_2\rangle}{\sqrt{1 - |\langle\psi_1|\psi_2\rangle|^2}}\right)|\psi_1\rangle + \left(\frac{1 - \sqrt{1 - |\langle\psi_1|\psi_2\rangle|^2}}{\sqrt{1 - |\langle\psi_1|\psi_2\rangle|^2}}\right)|\psi_2\rangle. \tag{2.32}$$

2.2 Application to Optical Coherent States

An important example of a binary state discrimination situation, and the one considered in this thesis, involves optical coherent states of the electromagnetic field [18]. The theory of quantum electrodynamics tells us that a monochromatic optical field, with a well-defined wavevector $\vec{k}$, can be treated as a harmonic oscillator with the Hamiltonian

$$\hat{H} = \hbar\omega \left(\hat{a}^\dagger \hat{a} + \frac{1}{2} \right), \tag{2.33}$$

where $\omega = c|\vec{k}|$ is the optical frequency. The field creation operator $\hat{a}^\dagger$ increases the number of quanta (photons) of electromagnetic energy in the optical mode by $\Delta E = \hbar\omega$. Conversely, the field annihilation operator $\hat{a}$ reduces the energy by one photon. Quantum uncertainty in the electromagnetic field, in analogy to the harmonic oscillator, results from the fact that the creation and annihilation operators satisfy a canonical commutation relation $[\hat{a}, \hat{a}^\dagger] = 1$.

Energy eigenkets of the single-mode Hamiltonian span Fock space and are called number states or, appropriately, Fock states.

$$\hat{H}|n\rangle = E_n|n\rangle, \quad E_n = \hbar\omega \left(n + \frac{1}{2} \right), \quad n = 0, 1, 2, 3, \ldots \tag{2.34}$$

These can be viewed as states of the field where the energy—and therefore the number of photons—is known with zero uncertainty. The Hermitian quantum operator associated with the number of photons in the field is given by the product of the creation and annihilation operators,

$$\hat{N} = \hat{a}^\dagger \hat{a}, \tag{2.35}$$

and is simultaneously diagonalized by the number states, $\hat{N}|n\rangle = n|n\rangle$. Other states of the electromagnetic field mode can be expressed using the number states as a basis,

$$|\psi\rangle = \sum_{n=0}^{\infty} c_n |n\rangle. \tag{2.36}$$

This thesis is concerned with distinguishing between optical coherent states $|\alpha\rangle$, which are eigenstates of the field annihilation operator

$$\hat{a}|\alpha\rangle = \alpha|\alpha\rangle \tag{2.37}$$

A coherent state describes an optical field produced by an ideal laser, where the eigenvalue α is the complex-valued amplitude of the plane wave generated by the laser. A coherent state $|\alpha\rangle$ is represented in the infinite-dimensional Fock space by [18]

$$|\alpha\rangle = e^{-\frac{|\alpha|^2}{2}} \sum_{n=0}^{\infty} \frac{\alpha^n}{\sqrt{n!}} |n\rangle. \tag{2.38}$$

Since the optical coherent states are not eigenstates of the number operator $\hat{N} = \hat{a}^\dagger \hat{a}$, there is quantum uncertainty in the number of photons in the field. If one were to measure the number operator of an optical field in the coherent state $|\alpha\rangle$, the different number outcomes would be obtained according to a Poisson distribution. Fig. 2.1 shows such a distribution for a coherent state of amplide $|\alpha| = 1$. Notice that although the mean photon number $|\alpha|^2$ is 1, the outcome of the number operator measurement is highly likely to be 0. A coherent state fitting a Poisson distribution,

$$\mathbb{P}(n) = \langle \alpha | \hat{a}^\dagger \hat{a} | \alpha \rangle \tag{2.39}$$

$$= \frac{|\alpha|^{2n}}{n!} e^{-|\alpha|^2}, \tag{2.40}$$

has a mean and variance of $|\alpha|^2$. That is to say, $|\alpha|^2$ is the mean number of photons that would be detected for a laser field described by the coherent state $|\alpha\rangle$, meaning that the laser power measured in a time-interval τ is related to the coherent state amplitude by

$$P = \frac{\hbar\omega|\alpha|^2}{\tau}. \tag{2.41}$$

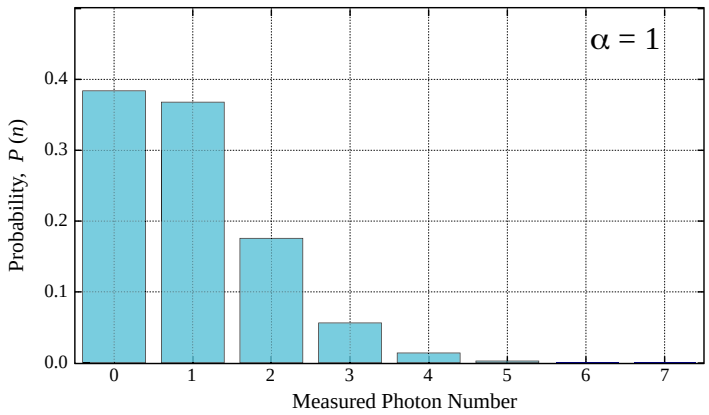

Figure 2.1: *Poissonian photon counting statistics for a single mode optical field in a coherent state with amplitude $\alpha = 1$, corresponding to an average of one photon in the laser field.*

2.2.1 Optical Displacements

It turns out that coherent states can easily be described as the vacuum state, $|0\rangle$, shifted by a *displacement operator*. In quantum optics, the displacement operator is defined as [18]

$$\mathcal{D}[\beta] = e^{\beta\hat{a}^\dagger - \beta^*\hat{a}}, \tag{2.42}$$

where $\hat{a}^\dagger$ and $\hat{a}$ are the raising and lowering operators, respectively. $\mathcal{D}[\beta]$ is a unitary operation and has the effect of transforming the annihilation operator by a scalar, represented in the Scrhödinger picture by

$$\mathcal{D}[\beta]^\dagger \hat{a} \mathcal{D}[\beta] = \beta\hat{a}. \tag{2.43}$$

It follows that the displacement operator transforms coherent states by shifting their amplitude [18]:

$$\mathcal{D}[\beta]|\alpha\rangle = |\alpha + \beta\rangle. \tag{2.44}$$

The physical process that best displays the effect of such an operation is interfering two coherent states, $|\alpha\rangle$ and $|\beta\rangle$, at a beam splitter. This provides a way to shift the amplitude and phase of a coherent state.

2.3 Binary Coherent State Discrimination

The number operators $|n\rangle$ are orthogonal, $\langle n|m\rangle = \delta_{nm}$, but coherent states are not. Thus, if the two candidate states in our alphabet are coherent states, then we cannot perfectly decide which state was handed to us; the quantum limit of error derived above is the best we can achieve. So, we are given one of two possible coherent states, $|\alpha_1\rangle$ and $|\alpha_2\rangle$, and asked to identify the secret state.

Thus, our alphabet can be displaced to the equivalent problem of distinguishing between $|0\rangle$ and $|\alpha\rangle$, where

$$|0\rangle = \mathcal{D}[-\alpha_1]|\alpha_1\rangle \quad \textit{and} \quad |\alpha\rangle = \mathcal{D}[-\alpha_1]|\alpha_2\rangle = |\alpha_2 - \alpha_1\rangle. \tag{2.45}$$

It is somewhat ridiculous to put it this way, but our "binary optical coherent state discrimination" problem is reducible to asking the question: Hey, is the light on or off?

2.3.1 The Shotnoise Error Probability

Let's look at this from an experimental point of view. What can we physically do to this unknown state to learn more about its identity? Our arsenal of laboratory measurement techniques basically amounts to two things: quadrature detection and photon counting. Quadrature detection is the name given to a variety of interferometric measurements that generally focus on determining the phase of a coherent state through the "quadrature operator" $\hat{Y} = i(\hat{a} - \hat{a}^\dagger)/2$ [18]. Photon counting implements a measurement of the number operator $\hat{N} = \hat{a}^\dagger\hat{a}$ to determine the number of photons in a laser field.

If we are merely trying to identify whether we have the vacuum state or the coherent state, photon counting seems like most viable experimental technique. It is easily employed and we can adopt a simple hypothesis testing procedure: if we receive a photon click, we say the state is $|\alpha\rangle$; if we do not, we say the state is $|0\rangle$. What is the probability that we are wrong if we proceed in this fashion? Referring to Eq. (2.5), the probability of error is given by

$$\mathbb{P}_E = \mathbb{P}(0|\alpha)p_\alpha + \mathbb{P}(\alpha|0)p_0. \tag{2.46}$$

Presumably, p_α and p_0 can be any value such that $p_\alpha + p_0 = 1$, but we are only concerned with the case of equal probability, $p_\alpha = p_0 = \frac{1}{2}$. Looking at the conditional probabilities above, we can use our testing policy to make some evaluations. The second term indicates the error that would occur if we mistakenly identify the vacuum state as $|\alpha\rangle$. But, assuming our photon counter is perfect, the vacuum would produce zero clicks and we would never misidentify it. We can now apply the Born rule and calculate the probability of error involved in photon counting:

$$\begin{aligned}
\mathbb{P}_E &= \frac{1}{2}\mathbb{P}(0|\alpha) + 0 && (2.47)\\
&= \frac{1}{2}|\langle 0|\alpha\rangle|^2 && (2.48)\\
&= \frac{1}{2}e^{-\frac{|\alpha|^2}{2}}e^{-\frac{|\alpha|^2}{2}} && (2.49)\\
&= \frac{1}{2}e^{-|\alpha|^2}. && (2.50)
\end{aligned}$$

This probability of error, called shotnoise, arises as a result of the fact that $|\alpha\rangle$ is a superposition of all number states in Fock space. Thus, it is possible for our counter to see no

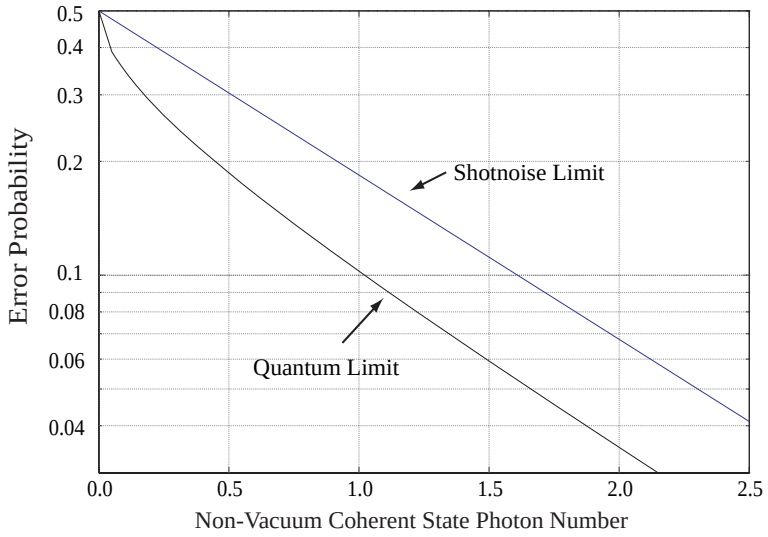

Figure 2.2: *Comparison of the quantum limit and shotnoise error probabilities for discriminating between two optical coherent states, $|0\rangle$ and $|\alpha\rangle$ as a function of the mean photon number $|\alpha|^2$.*

clicks, even when light is present, and we can mistake our coherent state for the vacuum. Clearly, this error is larger for smaller photon numbers, $|\alpha|^2$, which agrees with our intuition provided by Poisson statistics. If the photon number is large, there is small probability that the outcome will be zero clicks.

2.3.2 The Quantum Limit

Shotnoise is sometimes incorrectly referred to as a quantum limit [1, 8]. Let's look at the expression for the Helstrom bound in this case and see that it is smaller than the shotnoise. From Eq. (2.31),

$$p_H = \frac{1}{2}\left(1 - \sqrt{1 - 4\frac{1}{2}\frac{1}{2}|\langle 0|\alpha\rangle|^2}\right) \tag{2.51}$$

$$= \frac{1}{2}\left(1 - \sqrt{1 - e^{-|\alpha|^2}}\right). \tag{2.52}$$

Plotted in Fig. 2.2, the two curves are obviously different—for instance, at a mean photon number of one, the true quantum limit is nearly twice as small as the value of the shotnoise.

Remember, however, that this true quantum limit was determined by minimizing over all allowable POVMs. This means that the basis in which we need to make the measurement

is not necessarily convenient. According to what was found earlier, Eq. (2.32), we need to construct a basis for measurement that lies along

$$|-\rangle = \left(2\langle 0|\alpha\rangle - \frac{\langle 0|\alpha\rangle}{\sqrt{1-|\langle 0|\alpha\rangle|^2}}\right)|0\rangle + \left(\frac{1-\sqrt{1-|\langle 0|\alpha\rangle|^2}}{\sqrt{1-|\langle 0|\alpha\rangle|^2}}\right)|\alpha\rangle. \tag{2.53}$$

This Schrödinger cat-state basis for measurement involves a *superposition of coherent states*; the experimental viability of realizing such a measurement borders on the impossible, much less impractical. This is actually why shotnoise receives the quantum limit misnomer—it is largely accepted to be the feasible experimental limit.

Since the true quantum limit seems unreachable by a direct measurement, we need to employ more clever techniques if we hope to achieve it. This is where the theories of quantum feedback and control come into play.

Chapter 3

Closed-Loop Quantum State Discrimination

We want to minimize our probability of error and experimentally realize the true quantum limit; however, doing this through a direct cat-state measurement is ridiculously difficult. It has been forty years since Helstrom first performed the derivation of the true quantum limit discussed in the previous chapter, but no one has been able to physically construct an optimal basis in which to measure coherent states! Although it appears that constructing

$$|-\rangle = c_1(\alpha)|0\rangle + c_2(\alpha)|\alpha\rangle \tag{3.1}$$

will not be possible, the end goal of achieving the quantum limit of error is not necessarily limited by this fact. In place of the cat-state, we use real-time quantum feedback [10, 11, 13] to make a closed-loop measurement that gives us the best possible chance of guessing the correct identity of an unknown coherent state.

3.1 Closed-Loop Measurements

How is a closed-loop measurement different than standard POVMs? The answer is not very subtle, and it provides some insight as to why feedback may be highly useful in making a quantum measurement. Traditionally, a measurement in quantum mechanics is considered instantaneous—a quantum state is instantly transformed into its post-measurement state. The idea of using feedback admits that the measurement has a finite duration. During this

measurement, a quantum state can *both* evolve smoothly and change stochastically. In fact, any real measurement stipulates that this is case; an instantaneous measurement requires an infinite amount of energy and is therefore physically unrealistic.

In our specific case, the coherent states $|0\rangle$ and $|\alpha\rangle$ are optical pulses with a specified temporal extent τ and an average photon number. A measurement of such a pulse is made over time τ using a photon counter. From an instantaneous point of view, the result of the measurement is simply the number of clicks the counter produces over the time interval $[0, \tau]$, a measurement of the number operator. Clearly, however, these clicks occur at distinct moments in time. Something is lost if the measurement does not have a temporal duration. We, therefore, have a *measurement record*, $\Xi_{[0,\tau]}$, that tells us not only how many photons were counted, but *when*:

$$\Xi_{[0,\tau]} = (t_1, t_2, \ldots, t_n). \tag{3.2}$$

The idea of knowing when the clicks occurred shows that some extra information is hidden within an instantaneous description of photon counting: a temporal *history*. From an information perspective, feedback already appears to be on the right track to making a better measurement.

It also turns out that feedback is less demanding about the physical resources needed to implement it. This can be observed in a simple analogy from classical control theory. Consider an owner of a store who is only allowed to sell 10 units of a particular item in a day. If he has to prepare for an entire week in advance, he is forced by the worst-case scenario to order 70 units, and this does not guarantee that they will all be purchased. On the other hand, if he is allowed to examine his remaining stock and place an overnight order at the end of every day, he only has to order $10 - n$ units, where n is the number remaining at the end of the day. At the end of the week, the amount of excess resource provided by the store owner can vary drastically between the two cases—if no purchases are made, the owner either has 70 excess units on hand or 10. Thus, the simple act of him being able to examine his inventory during the week allows him to limit the expense on resources.

Similar to the analogy, open-loop POVMs are required to account for all possible outcomes of a measurement, making them physically demanding. A closed-loop feedback approach, meanwhile, can drive a quantum system during the measurement process to some-

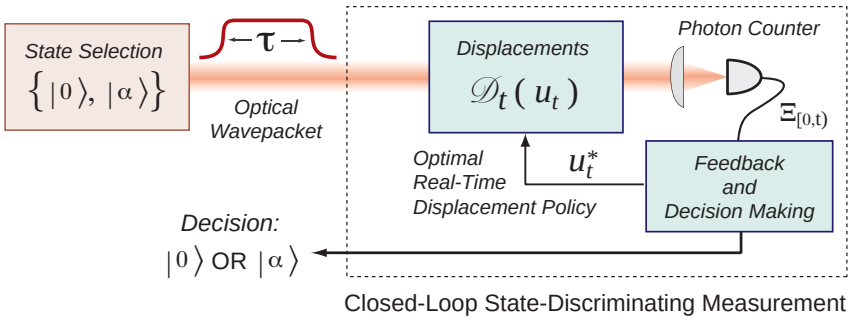

Figure 3.1: *Schematic of a closed-loop measurement that combines photon counting with feedback-mediated optical displacements to best determine the identity of an optical state.*

thing that is more readily feasible in the lab [13].

As admitted earlier, the toolbox of a quantum mechanic operating in the optical regime is quite limited: the most easily implemented laboratory operations are photon counting and displacements of coherent states. Fig. 3.1 shows a schematic that employs these two processes to make a closed-loop measurement for an optical state discrimination problem. The basic idea is to create smooth, unitary transformations of the quantum system while making a measurement. Optical displacements, which are unitary, are not only implemented simultaneously with photon counting, but are also dependent, through a feedback process, on the results of this measurement. Much like the store owner, we frequently examine our inventory by photon counting and decide what course of action through displacement should be taken. This idea is based on an approach suggested by Dolinar in 1973 [19] and has been refined and developed in light of quantum measurement theory in recent years [8].

But what determines our policy for implementing displacements? Well, it depends not only on current observations of the photon counting measurement, but also on the overall measurement history.

3.2 Determining an Optimal Policy

3.2.1 Feedback Hypothesis Testing Procedure

Since we are employing a feedback measurement with a time duration, we can introduce the concept of a probability that is constantly updating throughout the measurement. This

evolving probability is contingent upon the measurement history $\Xi_{[0,t]}$ as well as a history of the displacements performed on the system, u_t. This probability is updated according to Bayes' Rule,

$$\mathbb{P}\left(\psi|\Xi_{[0,\tau]}, u_{[0,\tau]}\right) = \frac{\mathbb{P}\left(\Xi_{[0,\tau]}|\psi, u_{[0,\tau]}\right)\mathbb{P}_0(\psi)}{\mathbb{P}(u_{[0,\tau]})}, \tag{3.3}$$

and describes the probability that $|\psi\rangle \in \{|0\rangle, |\alpha\rangle\}$ is the identity of the state, given both the displacement and measurement histories. If we want to maximize this, and thus increase our chance of being right, we need to maximize the conditional probability $\mathbb{P}(\Xi_{[0,\tau]}|\psi, u_{[0,\tau]})$. Since both the applied displacements and the measurement record are presumably known, selecting the state that maximizes the conditional probability is how state discrimination is performed. That is, if $\mathbb{P}(\Xi_{[0,\tau]}|\alpha, u_{[0,\tau]}) > \mathbb{P}(\Xi_{[0,\tau]}|0, u_{[0,\tau]})$, the identity of $|\psi\rangle$ is determined to be $|\alpha\rangle$, and vice versa. This process is often called a *maximum likelihood method*.

This is a straightforward way to discriminate between two states, but how are we supposed to evaluate these conditional probabilities? In order to do this easily, we need to exploit the fact that we are dealing with coherent states. The statistics of a coherent state ensure that it is a Poisson process; it follows that photon detection events are completely independent from one another. If we receive a click at time t, we are not any more or less likely to observe one at time $t + \delta t$. Thus the probability to see a click is constant over time; it can be calculated by considering the probability of detecting one photon during a $\delta t \ll 1$ time step. From the Poisson distribution fit by a coherent state $|\alpha\rangle$ over this time, the probability is found to be

$$\begin{aligned}
\mathbb{P}(1_{[0,\delta t]}) &= \frac{(|\alpha|^2\delta t)^1}{1!}e^{-|\alpha|^2\delta t} && (3.4)\\
&= |\alpha|^2\delta t\left(1 - |\alpha|^2\delta t + \frac{(|\alpha|^2\delta t)^2}{2!} + \ldots\right) && (3.5)\\
&\approx |\alpha|^2\delta t. && (3.6)
\end{aligned}$$

Now, the entire measurement duration can be broken up into N bins of time δt. Our measurement record $\Xi_{[0,\tau]}$ is composed of N *independent* events that each follow the probability given in Eq. (3.6). The conditional probability therefore simplifies to a product of the independent events:

$$\mathbb{P}(\Xi_{[0,\tau]}|\psi, u_{[0,\tau]}) = \prod_{i=1}^{N} |\psi + u_{t_i}|^2\delta t. \tag{3.7}$$

The calculation required to determine $|\psi\rangle$'s identity is now easily implemented. However, this only properly describes our hypothesis testing procedure for a closed-loop measurement if we know what u_t is!

3.2.2 Optimal Displacement

An optimum displacement policy, $u_t^\star$ is determined using a technique from control theory [20]. At every point in time, $t = [0, \tau]$, of the measurement, the amplitude of displacement is chosen so that the probability of error is minimized over the remaining measurement time $(t, \tau]$. When these are all combined, the time-additive analog of the traditional probability of error, Eq. (2.46), is created [8]. This is what needs to be minimized:

$$\mathbb{P}_{\mathrm{E}}[u_t] = \frac{1}{2}\int_0^\tau dt\,\left[\mathbb{P}(\alpha|0, u_{[0,t]}) + \mathbb{P}(0|\alpha, u_{[0,t]})\right]. \tag{3.8}$$

The conditional probabilities describe choosing the wrong state given the displacement history $u_{[0,t]}$. Minimizing this error is very different from what was previously done because this demands that the error is minimized at *all times* during the closed-loop measurement, not just at the end of an "instantaneous" measurement.

The expression is complicated, but it looks very similar to the action functional encountered in Lagrangian mechanics. In fact, the analogy works quite well because we are invoking the calculus of variations. Instead of finding the path of least action, as is done in Lagrangian mechanics, we are minimizing the probability of error. Minimization is solved by means of a partial differential equation called the Hamilton-Jacobi-Bellman equation; this recently was accomplished using modern optimal control theory [8], and the solution is

$$u_t^\star(n_{[0,t)}) = \frac{\alpha}{2}\left(\frac{e^{i\pi(n_{[0,t)}+1)}}{\sqrt{1-e^{-\bar{n}_\alpha t/\tau}}} - 1\right). \tag{3.9}$$

Applying this displacement amplitude analytically achieves the quantum limit of error for optical state discrimination, Eq. (2.31).

3.3 Interpreting the Optimal Solution

Eq. (3.9) is a displacement that alternates in time between two curves based on received photon counts $n_{[0,t)}$. One curve represents an odd number of registered clicks while the other

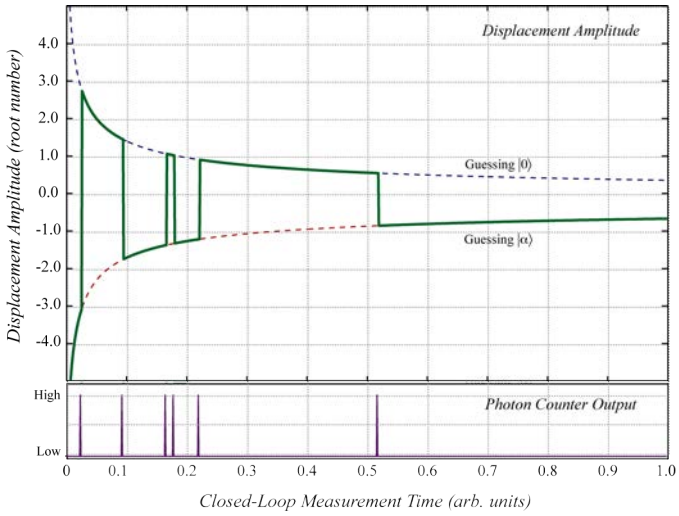

Figure 3.2: *The optimal displacement, $u_t^\star$, for a simulated trajectory alternates, with every detection of a photon, between two waveforms.*

an even number such that

$$u_t^\star(\text{odd}) = \frac{\alpha}{2}\left(\frac{1}{\sqrt{1-e^{-\bar{n}_\alpha t/\tau}}} - 1\right), \quad u_t^\star(\text{even}) = \frac{\alpha}{2}\left(\frac{-1}{\sqrt{1-e^{-\bar{n}_\alpha t/\tau}}} - 1\right). \tag{3.10}$$

Clearly, the odd case is strictly positive and the even strictly negative, while the difference between their magnitudes is $|u_t^\star(\text{even})| - |u_t^\star(\text{odd})| = \alpha$. Notable features of these curves are that they both start out at $t = 0$ with infinite magnitudes, and as $t \to \infty$, $u_t^\star(\text{odd})$ converges to 0 and $u_t^\star(\text{even})$ converges to $-\alpha$.

A very convenient consequence of these optimal displacements is an easy process of state discrimination. The conditional probability $\mathbb{P}(\Xi_{[0,\tau]}|\psi, u^\star_{[0,\tau]})$ is maximized when we make the following association: if we are currently applying the even displacement, our hypothesis is that the coherent state is $|\alpha\rangle$, and viceversa for the odd displacement and $|0\rangle$. Thus, when we apply the displacements of Eq. (3.9), we simply have to count the number of clicks produced by our photon counter to best determine the identity of $|\psi\rangle$. Since $u_t^\star$ stipulates that we start out with the belief that the state is $|\alpha\rangle$, our final decision is as follows: an odd number of clicks implies $|\psi\rangle = |0\rangle$; an even number of clicks implies $|\psi\rangle = |\alpha\rangle$.

A simulation created in Matlab demonstrates the process of switching between curves, and thereby hypotheses, each time a photon click is received. Plotted in Fig. 3.2 is the simulation for a single measurement trajectory which alternates between curves and ends up with the conclusion that the provided state was $|\alpha\rangle$. With this trajectory in mind, it

is appropriate to discuss some intuition about why this optimal solution works. We have implemented a displacement to push the quantum state to being more measurable by a photon counter, implying that we have displaced it to vacuum. Every time we observe a photon, we decide that we are doing a bad job of this negation. After all, that is what a photon counter measures efficiently—the difference between vacuum and not vacuum. This is precisely why the curve with value near $-|\alpha|$ at the end of the measurement is associated with the $|\alpha\rangle$ hypothesis: If we are right, then the photon counter will be very unlikely to produce a click. The same holds true for the opposite case as well.

The simulation that is used to create the trajectory plot is also applied to a statistical ensemble of trajectories, determining the correctness of guesses made using closed-loop feedback. A comparison is made between the simulated data and the quantum probability of error in Fig. 3.3, indicating that this feedback process does indeed mimic the statistics of the optimal cat-state measurement. Now, we just need to realize this experimentally.

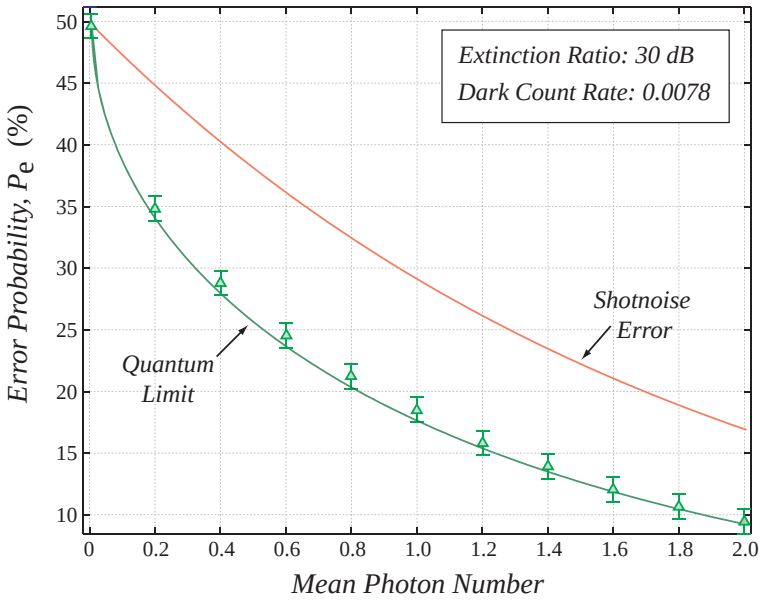

Figure 3.3: *Simulated data for the probability of error resulting from a closed-loop discrimination between two quantum states $|\alpha\rangle$ and $|0\rangle$ as a function of the mean photon number, $|\alpha|^2$*

Chapter 4

The Experiment

We now have an optimal solution given the advantage of a closed-loop adaptive measurement. Although the theory behind its derivation is complicated, laboratory implementation of the solution involves only displacement of the quantum state, photon counting, and manipulation of displacement amplitudes. These are all relatively easy to do; the following pages discuss the physical realization of a closed-loop quantum coherent state discrimination.

4.1 Apparatus

4.1.1 Enabling Displacements

Fig. 4.1 shows a schematic of the laboratory setup. Infrared light from an 852 nm diode laser is incident on a Mach-Zender interferometer that terminates at a silicon avalanche photodiode (APD). The source laser is split at the initial fiber beamsplitter (FBS1) to produce two separate optical fields. The upper arm of the interferometer provides the quantum state that we are investigating, while the lower arm acts as a *local oscillator* that displaces the quantum state as they couple into the interferometer's terminating beamsplitter (FBS2). It is worth noting that all elements in the interferometer use polarization-maintaining fiberoptics, ensuring that excellent mode-matching and good phase stability between the arms are achieved. This makes optical implementation of displacements on our quantum state much easier.

Each arm of the interferometer features a fiber-coupled intensity modulator (FIM). This

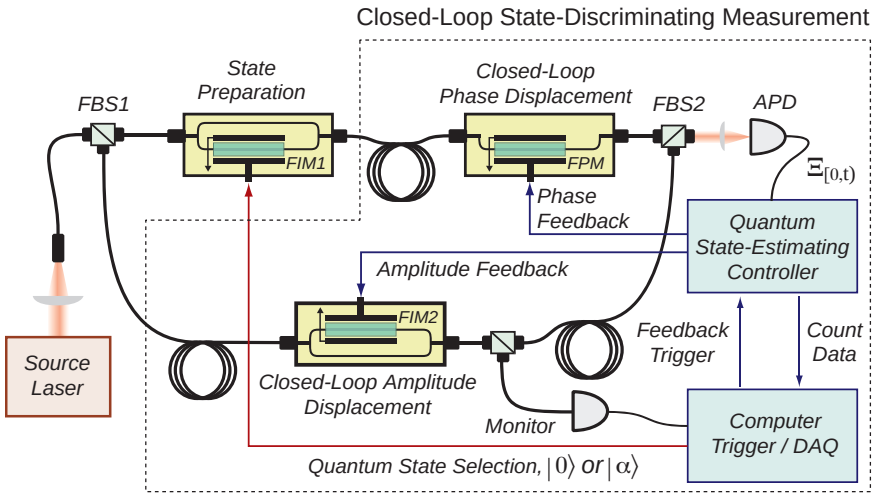

Figure 4.1: *Schematic of laboratory implementation of the closed-loop measurement—the quantum state is prepared at FIM1, while the contents of the dotted region compose the feedback controller.*

device can alter the amplitude of an incoming field through the use of an electro-optical crystal and an interferometer of its own. Placed in one of the arms of the internal interferometer, the crystal's index of refraction changes with an applied electric field. Since the crystal lies between two capacitor plates, applying a field across the crystal is equivalent to applying a voltage. Thus, through a voltage, a phase difference is created and a change in amplitude is induced. The fiber-coupled phase modulator (FPM) in the upper arm of Fig. 4.1 operates similarly, except it is not equipped with its own interferometer. It merely alters the path length for the field in that arm.

FIM1, in the upper arm, is where the to-be-discriminated quantum state is prepared; we can control the amplitude via an input voltage. The rest of the setup, however, is devoted to the closed-loop measurement, as indicated by the dotted region in the figure: FIM2 is used to control the amplitude of the local oscillator while the FPM regulates the phase difference between the local oscillator and the quantum state. It is through these two modulators that we will be able to produce the prescribed local oscillator curves given by Eq. (3.9).

Coherent states in this experiment are constructed as square optical pulses that have a duration of $\tau = 20$ μs and amplitude $|\alpha|$. The feedback enabled measurement occurs over this 20 μs time frame. This allows us to run many trajectories and obtain decent statistics.

4.1.2 Control Electronics

All voltages applied to the modulators are governed by a computer equipped with high-speed digital signal processing electronics. The computer can produce feedback at a bandwidth of about 30 MHz and actually controls all elements of our apparatus: it provides a voltage that stipulates the selection of our quantum state, creates waveforms to be transmitted to the modulators during the feedback process, triggers the photodiode, and records photon counter clicks during the measurement window. The computer's electronics do not have the capability to drive large voltages, but this is not a requirement of our setup. Since the electro-optic modulators used in our experiment are fiber coupled, they can utilize a smaller crystal whose index of refraction is to be altered. In this case, an equivalent electric field, and thereby change in path length, is achieved with a smaller voltage, on the order of 100 mV. This means that our control of amplitudes and phases via the modulators can be very precise—yet another strength to using an all-fiber setup.

The business of switching waveforms and phases, which is required by the optimal solution u_t, is controlled outside the computer. Four voltage channels are sent from the computer into two separate switches: The first switch takes two channels that act as changing amplitude waveforms to be sent to FIM2; the second takes two channels that determine the appropriate phase displacement at the FPM. The appropriate amplitude and phase, associated with the $|\alpha\rangle$- and $|0\rangle$-case policies, are implemented simultaneously. Every click that is received by the photon counter is then propagated electronically to the digital switches, and the current policy is updated to become the alternative. This happens exactly as simulated in Fig. 3.2.

All the components of our prescribed, real-time quantum feedback are in place; however, some classical feedback electronics are also necessary. The fiberoptic construction of our apparatus has some noise effects—the fiber is quite sensitive to vibrational and thermal noise. Because of this, our interferometer has noise-induced path length variations that we need to eliminate. We use standard classical control theory to create an error signal and lock the path length of our interferometer [21]. In addition, the modulators lose their calibrations, described below, due to their sensitivity to fluctuations in temperature. They have been thermally stabilized in a similar classical control approach.

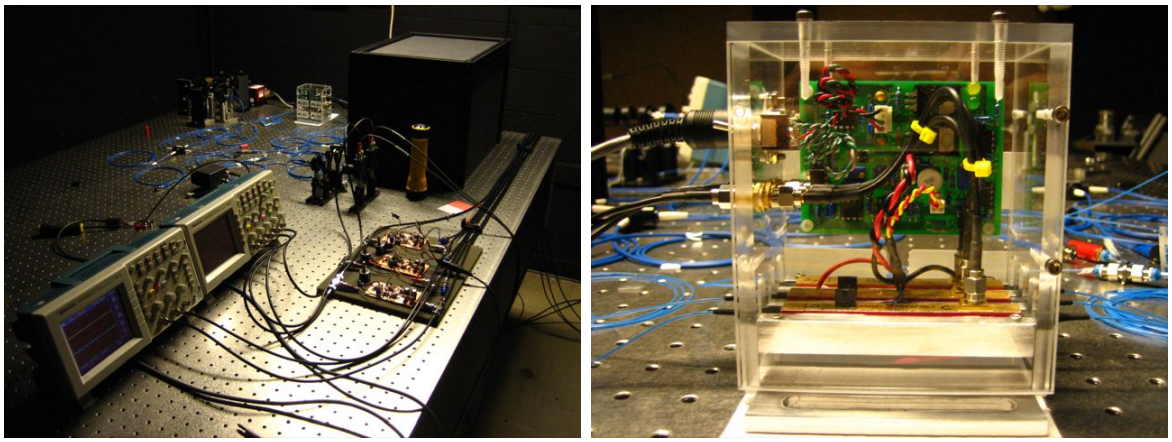

Figure 4.2: *Photographs of laboratory setup. The overall apparatus is pictured on the left, and the temperature-stabilized, fiber-coupled modulators on the right.*

This is the entirety of the physical apparatus: the overall Mach-Zender structure, the amplitude and phase modulators, the feedback control provided by the computer, and the control electronics. Fig. 4.2 shows two pictures of our actual apparatus with the control electronics in place. The APD is inside the black box of the left-hand picture and the blue objects are coils of fiberoptical cable. The picture on the right, meanwhile, features the temperature-controlled housing of the electro-optical modulators; the small circuit is the control servo and the three narrow gold structures at the base are the modulators.

4.2 Calibrations

In order to utilize the modulators, we need to be certain that input voltages yield the desired effects. The calibration procedure for the intensity modulators is simple: After isolating the modulator by disabling the interferometer, we input a range of voltages, count the number of clicks that our photon counter registers over the 20 μs pulse, and average over 100,000 trajectories. The resulting plot of data is not included, but looks much like Fig. 4.4. Since the voltage relates linearly to the phase delay produced by the crystal, it makes sense that mean photon number plotted against the applied voltage will be sinusoidal. We are able to fit these data and invert the relationship. As a final step, we attempt to produce a mean photon number $|\alpha|^2$ by applying the calibrated voltage. Fig. 4.3 shows a parity plot, which demonstrates our success at preparing desired amplitudes, for each of our intensity

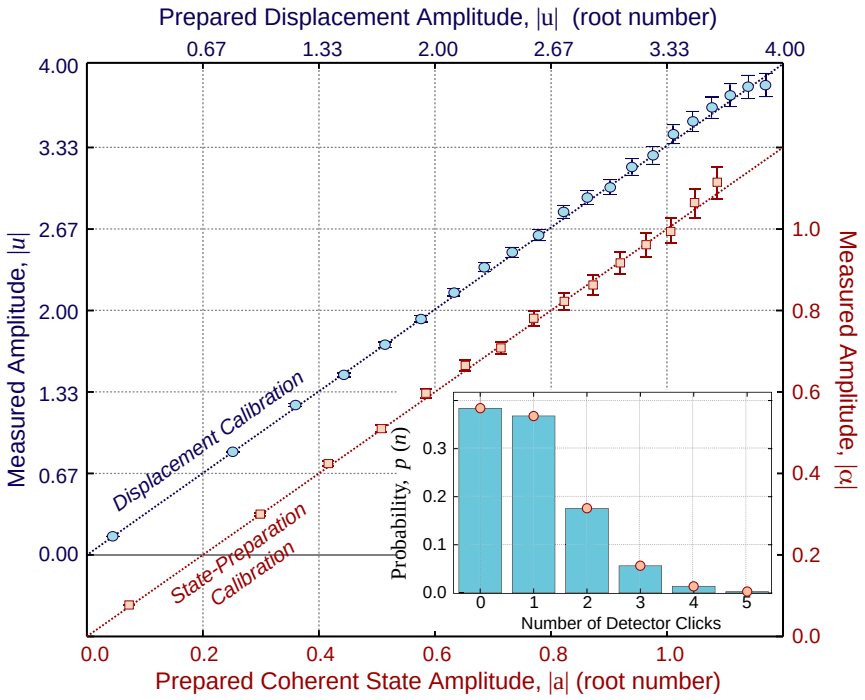

Figure 4.3: *These parity plots demonstrate our ability to accurately produce amplitudes using the intensity modulators. The top curve is FIM1 and the bottom is FIM2. The inset plot, meanwhile, demonstrates the Poisson statistics of a coherent state.*

modulators.

Also worth noting in Fig. 4.3 is the inset plot. This features the counting statistics of a prepared state, where $|\alpha|^2$ is app 1. We expect the statistics of a coherent state to be Poissonian; it is reassuring that for a Poisson fit of the data we find $\chi^2 - 1 < 10^{-6}$. This means that our produced quantum coherent states are indeed limited by quantum mechanics.

After setting both of the intensity modulators to the same amplitude and reconnecting the interferometer, we now can calibrate the FPM. A plot of relative interferometer phase difference is generated by applying a range of voltages to the phase modulator. Fig. 4.4 shows that we achieve a full range of phase differences. Initially a plot of mean photon number versus modulator voltage, this curve has a maximum when the two arms of the interferometer are in phase. We thus define this maximum point as having zero relative phase; the minimum point, on the other hand, occurs when the two arms are completely out of phase. V_π is defined to be the voltage between the in- phase and out-of-phase cases. Thus, we know exactly the change in voltage needed to switch the phase as stipulated by

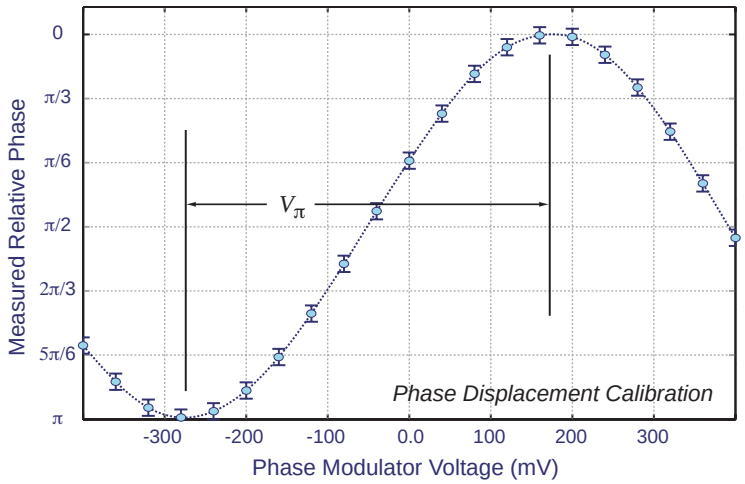

Figure 4.4: *This phase calibration allows us to implement any relative phase between the interferometer arms. V_π is the voltage difference required to achieve a full range of phase differences.*

our optimal solution.

With calibrations complete, we are ready to implement the optimal solution $u_t^\star$; however, there are some experimental issues that we need to consider.

4.2.1 Limitations and Imperfections

Since this is an actual physical implementation, certain aspects of our apparatus are not ideal. First of all, our photon counter is not perfect. Even in complete isolation from any source of light it will randomly detect something and produce a click. This rate, for the time frame in which we are interested, is $\bar{n}_0 = 0.0078$ (which translates to about 40 counts per second) and is referred to as a *dark count rate*. Thus, there is always a small probability that our photon counter will produce a click.

Another cause for concern is the limited amplitude range provided by our modulators, specifically in FIM1. A feature of these modulators in real life is that they cannot achieve perfect destructive interference. A measurable quality called the extinction ratio can qualify how effective a particular modulator is at making an optical state vanish. For our purposes, the extinction ratio, r_e, is given in decibels by

$$r_e = 10 \log_{10} \left(\frac{n_{max}}{n_{min}} \right), \tag{4.1}$$

where n_{max} is the largest number of photon counts in a certain time window and n_{min} is the smallest. These correspond to no destructive interference and fully destructive interference, respectively.

In our apparatus, FIM1 is of particular concern because it acts as the amplitude modulator for the local oscillator. This means that it needs to be able to produce small photon numbers, at or near the darkcount rate. On the other hand, the optimal solution calls for the waveform to begin with a *very large* amplitude. Since we are more concerned with having the ability to achieve the vacuum, the maximum amplitude of our light is limited such that it is no longer optimal. We use our modulator with the highest extinction ratio as FIM1. For this modulator, r_e is around 33, but what matters more is that we are limited to producing mean photon numbers between $n_{min} \sim 0.008$ and $n_{max} \sim 15.8$.

The simulations discussed in Chapter 3 are designed to incorporate the limitations of the modulators and APD. When the appropriate values are included, results show that their effects are limited. We should still be able to approach the quantum limit given the limitations of our apparatus.

A final detail that should be discussed is that of efficiency. Since we displace the quantum state in question by means of a beamsplitter, we introduce some loss in the efficiency of our apparatus. The coupling beamsplitter that is used in our apparatus is fifty percent transmissive and fifty percent reflective. Because of this, half of the quantum state that has come our way is lost—reflected into nothingness. The efficiency η automatically drops to 0.5 because of this and is subject to other optical losses as well. However, since we conduct our experimental feedback and calibrations based on photons received at the counter, this inefficiency does not affect us. It factors out entirely; the shotnoise limit, quantum limit, and our error calculations all possess the same efficiency. We can still expect our closed-loop calculation of the probability of error to approach the limit that quantum mechanics imposes on our apparatus.

4.3 Results

Before attempting to produce a closed-loop result, we should verify that our apparatus is capable of producing results in agreement with the shotnoise probability of error. This involves just photon counting of the prepared coherent state. Sampling with equal probability from $|0\rangle$ and $|\alpha\rangle$, our goal is to identify which state was provided. We adopt the hypothesis testing procedure outlined in Chapter 2: if the photon counter produces a click, we say the unknown state is $|\alpha\rangle$; if not, it's $|0\rangle$. We then can compare our decision with the state that was actually prepared to determine if an error occurred. The red squares in Fig. 4.6 are data points of 100,000 trajectories with $0 \leq |\alpha|^2 \leq 1$. Our data agree very well with the shotnoise limit of error; we have a discrepancy of $\chi^2 - 1 = 1.13 \times 10^{-5}$. This demonstrates that the dark count rate of the APD does not inhibit our ability to count photons effectively.

Fig. 4.5 shows a single trajectory of a closed-loop measurement when the coherent state is $|\alpha\rangle = |0.02\rangle$. The square root of the mean photon number taken over many trajectories is displayed in (**a**) as $|\alpha|$. The displacement $u_t^\star$, provided by the local oscillator, is also shown,

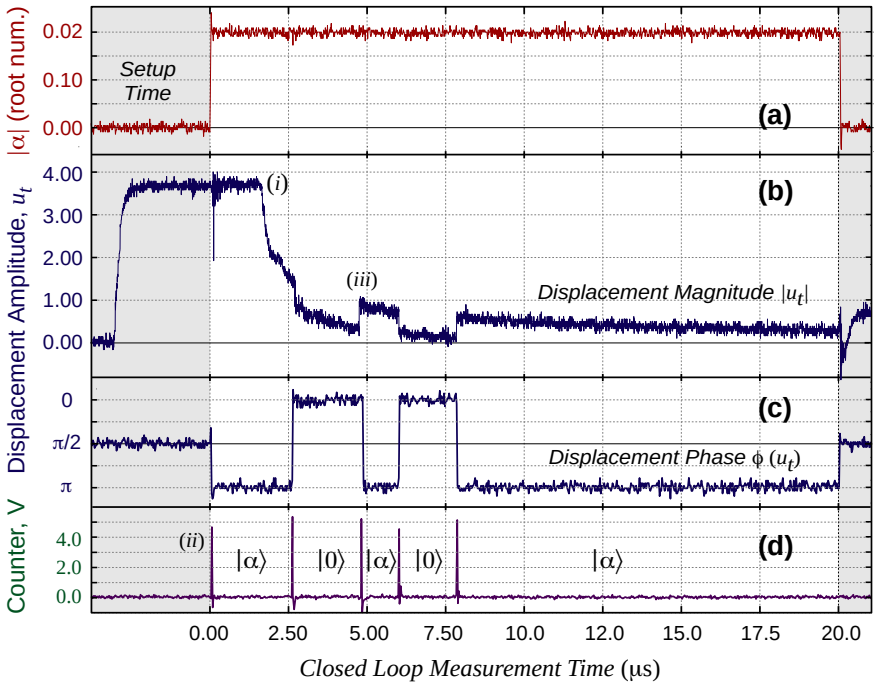

Figure 4.5: *An oscilloscope trace of the output of FIM2 demonstrates the laboratory apparatus' ability to alternate between waveforms with each photon detection.*

with (**b**) showing its magnitude and (**c**) its phase. The final panel, (**d**), is the output of our photon counter. With each received count, our hypothesis about the identity of the state changes. At the end of this particular trajectory, we predict the unknown state to be $|\alpha\rangle$ and are correct in that prediction.

For the most part, Fig. 4.5 looks like our optimal solution says it should, but a few details should be discussed. As mentioned before, we are limited to a finite amplitude at (*i*) when the theorized $u_t^\star$, from Eq. (3.9), clearly calls for a much larger amplitude. Notice that the magnitude at this point is the maximum allowed by r_e, just short of $|4|$, which would yield a mean photon number of 16. At the point labeled (*ii*), the computer gates on the APD as well as the voltage output to the modulators. This spike at $t = 0$ is not a real detection event—it is simply a timing signal that declares the photon counter is on. Finally, as (*iii*) indicates, there appears to be a rise-time in the changing displacement magnitude. This is only an effect of the photodiode that is monitoring this amplitude; it is not an actual physical feedback process.

After running 100,000 trajectories like this one for several coherent state magnitudes, we are ready to look at some data. The process for making our guess remains the same as that outlined in section 3.3: since we start with the belief that the unknown quantum state is $|\alpha\rangle$, an odd number of clicks corresponds to thinking we were given $|0\rangle$ and an even number of clicks to $|\alpha\rangle$. For each trajectory, we compare our guess with the state that was actually prepared; the probability of error is simply the number of times we were wrong divided by the total number of trials. The blue circles in Fig. 4.6 are the results of a particular set of data analyzed in this manner. All data points for $|\alpha|^2 \leq 1$ fall below the shotnoise limit of error; however, for mean photon numbers larger than a half, our data pulls away significantly from the true quantum limit.

It appears that not being able to perfectly mimic the curves of $u_t^\star$ greatly affects our ability to reach the quantum limit. But, there is a problem! Since we were not able to mimic the displacements required by the optimal solution, we should not be restricted to making our decision based only on the number of photon counts—equivalent to basing our decision on the theoretical displacement history. With thanks to a suggestion from H.M. Wiseman, we re-evaluate our data, this time using the *actual* displacement history. This history corresponds

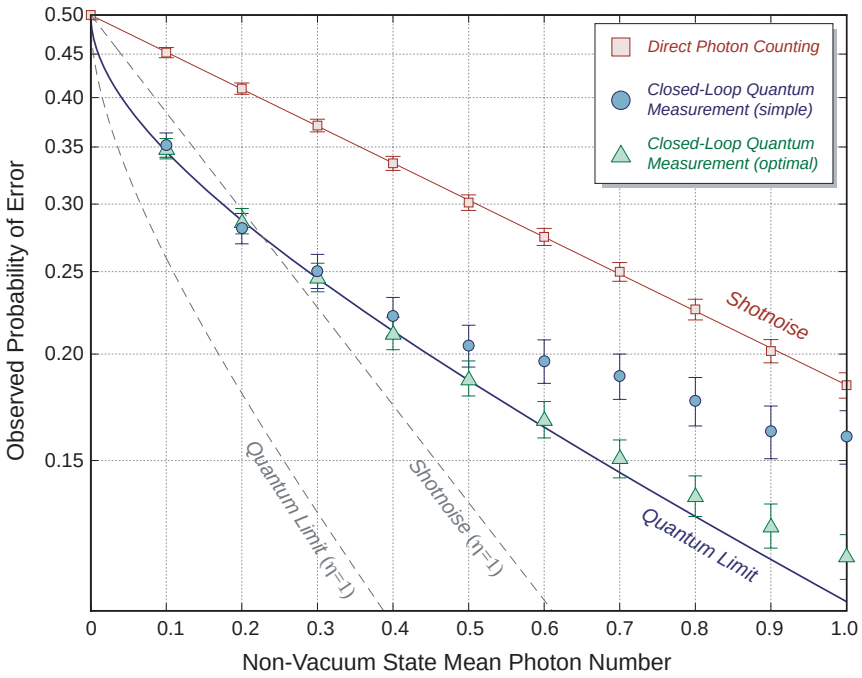

Figure 4.6: *A demonstration of the probability of error experimentally achieved by the apparatus of Fig. 4.1. The squares are obtained through direct photon counting and are shotnoise-limited; the circles represent the first analysis of a closed-loop measurement with* $0 \leq |\alpha|^2 \leq 1$*; the triangles represent a second, more accurate analysis, as suggested by H.M. Wiseman.*

to trajectories like the plot of Fig. 4.5 and not $u_t^\star$, the optimal version. We, therefore, return to determining which quantum state maximizes the conditional probability $\mathbb{P}(\Xi_{[0,\tau]}|\psi, u_{[0,\tau]})$, only using the appropriate $u_{[0,\tau]}$. We do not end up with the convenient counting policy as outlined in section 3.3, but can determine the most likely candidate state nonetheless. Analyzed in this manner, the exact same data from above becomes the green triangles in Fig. 4.6. Our procedure nearly achieves the quantum limit over all photon numbers tested.

Chapter 5

Conclusions

The data in Fig. 4.6 demonstrates a quantum state discrimination measurement that successfully outperforms the shotnoise probability of error and approaches the true limit imposed by quantum mechanics.

This was done not through constructing an optimal cat-state measurement basis, but rather by utilizing a real-time, closed-loop quantum feedback measurement. During a counting measurement, displacements of a coherent state are performed to optimize the chance of correctly identifying it. By performing quantum feedback, no longer do all possible statistical outcomes need to be considered to make an optimal quantum measurement. A closed-loop measurement is thus less costly to implement in the laboratory, without losing any theoretical optimality.

This experiment demonstrates the first sub-shotnoise measurement of probability of error and serves as a proof-of-principle that quantum feedback is a viable means to emulating optimal quantum measurements in real life.

My personal effort on this project includes mostly experimental aspects, since the theory discussed in the first three chapters was already in place. I wrote and ran a simulation code, included as an appendix, to help aid in designing the experimental apparatus; I performed the optical procedures involved in creating and manipulating the coherent states; and I designed and built some of the required control electronics. Additionally, I assisted Rob Cook in writing the Matlab code that interfaced with the experiment by managing counting and displacement processes, calibrating the electro-optic modulators, and collecting and

graphically interpreting data.

I would like to thank JM Geremia and Rob Cook for inviting me to be a part of this project. They allowed me to take part in every portion of the experiment and ensured that I was an equal owner of the project and any decisions that were made. They were equally invaluable in helping me understand any physics involved, and I hope that the resulting clarity with which I view this project has been passed along accordingly by this thesis.

Bibliography

[1] C. A. Fuchs. *Distinguishability and Accessible Information in Quantum Theory*. PhD thesis, University of New Mexico, 1996. quant-ph/9601020.

[2] Michael Nielsen and Isaac Chuang. *Quantum Computation and Quantum Information Science*. Cambridge University Press, London, 2000.

[3] John von Neumann. *Mathematical Foundations of Quantum Mechanics*. Princeton University Press, Princeton, 1955.

[4] C. W. Helstrom. Detection theory and quantum mechanics. *Information and Control*, 10:254, 1967.

[5] C. W. Helstrom. *Quantum Detection and Estimation Theory*, volume 123 of *Mathematics in Science and Egineering*. Academic Press, New York, 1976.

[6] A. Peres and W. K. Wooters. Optimal detection of quantum information. *Phys. Rev. Lett.*, 66:1119, 1991.

[7] M. Sasaki and O. Hirota. Quantum decision scheme with a unitary control processs binary quantum-state signals. *Phys. Rev. A*, 54(4):2728, 1996.

[8] JM Geremia. Optimal discrimination of optical coherent states with imperfect detection. *Phys. Rev. A*, 70:062303, 2004.

[9] H. M. Wiseman and G. J. Milburn. Quantum theory of field-quadrature measurements. *Phys. Rev. A*, 47:642, 1993.

[10] Howard M. Wiseman and Gerard J. Milburn. All-optical versus electro-optical quantum-limited feedback. *Phys. Rev. A*, 49:4110, 1994.

[11] Andrew C. Doherty, Salman Habib, Kurt Jacobs, Hideo Mabuchi, and Sze M. Tan. Quantum feedback control and classical control theory. *Phys. Rev. A*, 62(1):012105, 2000.

[12] M. A. Armen, J. K. Au, J. K. Stockton, A. C. Doherty, and H. Mabuchi. Adaptive homodyne measurement of optical phase. *Phys. Rev. Lett.*, 89:133602, 2002.

[13] JM Geremia, John K. Stockton, and Hideo Mabuchi. Real-time quantum feedback control of atomic spin-squeezing. *Science*, 304:270, 2004.

[14] K. Kraus. *States, Efects, and Operations: Fundamental Notions of Quantum Theory*, volume 190 of *Lecture Notes in Physics*. Springer-Verlag, Berlin, 1983.

[15] A. Peres. Neumark's theorem and quantum inseparability. *Found. Physics*, 20:1441, 1990.

[16] C.W. Gardiner. *Quantum Noise*. Springer Verlag, 1991.

[17] A. C. Doherty, S. M. Tan, A. S. Parkins, and D. F. Walls. State determination in continuous measurement. *Phys. Rev. A*, 60:2380, 1999.

[18] R.J. Glauber. Coherent and incoherrent states of the radiation field. *Phys. Rev. Lett.*, 131(6):2766, 1963.

[19] S.J. Dolinar. Quarterly progress report. Technical Report 111, Research Laboratory of Electronics, MIT, 1973.

[20] Dimitri P. Bertsekas. *Dynamic Programming and Optimal Control*, volume 1. Athena Scientific, Belmont, Massachusetts, 2 edition, 2000.

[21] Robert L. Cook, Paul J. Martin, and JM Geremia. Optical coherent state discrimination using a closed-loop quantum measurement. *Nature*, 446:774, April 2007.

Appendix A

Matlab Simulation Code

This Appendix contains some example code, which was written to simulate the closed-loop state discriminating quantum measurement. The simulations include experimental imperfections like the optical modulator extinction ratio and the quantum efficiency and dark count rate of the photon counter. This code was used to help design the experimental apparatus and to aid in interpreting the resulting data.

```
% %%%%%%%%%%%%%%%%%%%%%%%%%%%%%%%%%
% simulateStatisticsMeasurement.m
% Simulate a measurement of the quantum error probability by
% performing Monte Carlo simulation of the quantum measurement

clear all;

    SignalProbability       = 0.5;
    TrajectoryCount         = 100000;
    PhotonNumberList    = [ .1 : .2 : 1 ];

    % %%%%%%%%%%%%%%%%%%%%%%%%%%%%%%%%%
    % Loop over signal coherent states (with different photon number)

    ErrorProbability = zeros( length( PhotonNumberList ), 1 );

    fprintf('Running Closed-Loop Measurement Simulation\n');
    for Index = 1 : length( PhotonNumberList )

        fprintf('    Photon number %1.1f (%4d of %02d)\t PError = ', ...
            PhotonNumberList(Index), Index,length(PhotonNumberList) );
```

```
        VerdictList = zeros( TrajectoryCount, 1 );

        StateList   = random( 'Uniform', 0, 1, TrajectoryCount, 1 ) ...
         > 0.75*SignalProbability;

        % %%%%%%%%%%%%%%%%%%%%%%%%%%%%%%%%
        % Loop over state discrimination measurement trajectories

        for TrajectoryIndex = 1 : TrajectoryCount

            [VerdictList(TrajectoryIndex) ] = ...
             closedLoopStateDiscrimination( ...
             StateList(TrajectoryIndex), ...
                   PhotonNumberList(Index), SignalProbability );
        end

        % %%%%%%%%%%%%%%%%%%%%%%%%%%%%%%%%
        % Compute the number of state discrimnation errors
        ErrorProbability(Index) = sum( VerdictList ~= StateList ) ...
         / TrajectoryCount;

        fprintf('%f\n',ErrorProbability(Index));

    end

    NumberList     = [ 0: 0.01 : max( PhotonNumberList ) ];
    HelstromLimit  = ( 1 - sqrt( 1 - ...
        4*SignalProbability*( 1-SignalProbability ) * ...
        exp( -NumberList ) ) ) / 2;
    ShotnoiseLimit = min( [SignalProbability 1-SignalProbability] ) ...
     * exp(- NumberList );

    figure( 1 );
    semilogy( PhotonNumberList, ErrorProbability, 'b*', ...
              NumberList, HelstromLimit, 'b', ...
              NumberList, ShotnoiseLimit, 'k');
    grid;
    set( gca, 'Ylim', [8E-2 0.5] );

% %%%%%%%%%%%%%%%%%%%%%%%%%%%%%%%%
% END

% %%%%%%%%%%%%%%%%%%%%%%%%%%%%%%%%
% closedLoopStateDiscrimination.m
%
% This function simulates the closed-loop quantum measurement
```

```
function [ Verdict ] = closedLoopStateDiscrimination( ...
                            SignalState, PhotonNumber, SignalProbability )

    p1 = SignalProbability + 0.01;
    p0 = 1 - p1;

    TimeList = linspace(0, 1, 200);

    SignalIntensity = SignalState * PhotonNumber;

    % %%%%%%%%%%%%%%%%%%%%%%%%%%%%%%%%
    % Compute the Local Oscillator Amplitude Gain Profile

    NumberData = TimeList * PhotonNumber;

    % %%%%%%%%%%%%%%%%%%%%%%%%%%%%%%%%
    % Compute the two Local Oscillator Intensity Waveforms

    LOGainData = ( 1 ./ sqrt( 1 - 4*p0*p1*exp( -NumberData ) ) - 1 ) / 2;
    LOIntensity(:,1) = (LOGainData+1).^2 * PhotonNumber;
    LOIntensity(:,2) = (LOGainData).^2 * PhotonNumber;

    % %%%%%%%%%%%%%%%%%%%%%%%%%%%%%%%%
    % Perform the Measurement

    [ClickData, LOAmplitude] = ...
     simulateMeasurement( SignalIntensity, LOIntensity );

    % %%%%%%%%%%%%%%%%%%%%%%%%%%%%%%%%
    % Determine the State Discrimination Outcome

    Verdict = not( mod( sum( ClickData ), 2 ) )';

return

% %%%%%%%%%%%%%%%%%%%%%%%%%%%%%%%%
% simulateMeasurement.m
%
% This measurement simulates a displaced photon counting detector

function [ClickData, LOAmplitude] =
simulateMeasurement( SignalIntensity, LOIntensity )

    MaxSignalIntensity = 2.0;
    MaxLOIntensity     = 11;

    MinSignalIntensity = 0.005;
```

```
    MinLOIntensity     = 0.02;

    DarkCountRate      = 0.0075;      % Detector Dark Count Rate
    PhaseNoise         = 100;       % Phase Noise in mRad

    SignalIntensity = min( SignalIntensity, MaxSignalIntensity );
    SignalIntensity = max( SignalIntensity, MinSignalIntensity );
    LOIntensity     = min( LOIntensity, MaxLOIntensity );
    LOIntensity     = max( LOIntensity, MinLOIntensity );

    SignalIntensity = SignalIntensity* (1+random('Normal',0,.1));
    LOIntensity     = LOIntensity*(1+random('Normal', 0, 0.1 ) );

    StateAmplitude = sqrt( SignalIntensity );

    TimeData  = linspace( 0, 1, length( LOIntensity ) );
    dt = TimeData(2) - TimeData(1);

    RData     = random( 'Uniform', 0, 1, length( TimeData ), 1 );
    ClickData = zeros( length( TimeData ), 1 );
    LOAmplitude = zeros( length(TimeData), 1 );

    Count = 0;

    TotalIntensity = zeros( size(TimeData) );

    for TimeIndex = 1 : length( TimeData )

        p = mod( Count, 2 );
        LOAmplitude(TimeIndex) = ...
         exp( i*pi*(p+1)) * sqrt( LOIntensity(TimeIndex,p+1) );
        TotalAmplitude = ( StateAmplitude + LOAmplitude(TimeIndex) );
        TotalIntensity(TimeIndex) = TotalAmplitude' * TotalAmplitude;

        if ( (TotalIntensity(TimeIndex)+DarkCountRate)*dt > ...
         RData(TimeIndex) )
            Count = Count + 1;
            ClickData( TimeIndex ) = 1;
        end

    end

return
```